

Received March 31, 2021, accepted April 11, 2021, date of publication April 28, 2021, date of current version May 14, 2021.

Digital Object Identifier 10.1109/ACCESS.2021.3076405

Identifiability of Control-Oriented Glucose-Insulin Linear Models: Review and Analysis

J. D. HOYOS¹, M. F. VILLA-TAMAYO¹, C. E. BUILES-MONTAÑO^{1,2,3}, A. RAMIREZ-RINCÓN^{4,5}, J. L. GODOY⁶, J. GARCIA-TIRADO⁷, (Senior Member, IEEE), AND P. S. RIVADENEIRA¹

¹Universidad Nacional de Colombia, Facultad de Minas, Grupo GITA, Medellín 050034, Colombia

²Hospital Pablo Tobón Uribe, Medellín 050034, Colombia

³Facultad de Medicina, Universidad de Antioquia, Medellín 050010, Colombia

⁴Clínica Integral de Diabetes, Medellín 050022, Colombia

⁵Facultad de Medicina, Universidad Pontificia Bolivariana, Medellín 050034, Colombia

⁶INTEC -CONICET, Santa Fe 3450, Argentina

⁷Center for Diabetes Technology, University of Virginia, Charlottesville, VA 22904, USA

Corresponding author: P. S. Rivadeneira (psrivade@unal.edu.co)

This work was supported by the Minciencias (Colombia) under Grant 110180763081.

ABSTRACT One of the main challenges of glucose control in patients with type 1 diabetes is identifying a control-oriented model that reliably predicts the behavior of glycemia. Here, a review is provided emphasizing the structural identifiability and observability properties, which surprisingly reveals that few of them are globally identifiable and observable at the same time. Thus, a general proposal was developed to encompass four linear models according to suitable assumptions and transformations. After the corresponding structural properties analysis, two minimal model structures are generated, which are globally identifiable and observable. Then, the practical identifiability is analyzed for this application showing that the standard collected data in many cases do not have the necessary quality to ensure a unique solution in the identification process even when a considerable amount of data is collected. The two minimal control-oriented models were identified using a standard identification procedure using data from 30 virtual patients of the UVA/Padova simulator and 77 diabetes care data from adult patients of a diabetes center. The identification was performed in two stages: calibration and validation. In the first stage, the average length was taken as two days (dictated by the practical identifiability). For both structures, the mean absolute error was 16.8 mg/dl and 9.9 mg/dl for virtual patients and 21.6 mg/dl and 21.5 mg/dl for real patients. For the second stage, a one-day validation window was considered long enough for future artificial pancreas applications. The mean absolute error was 23.9 mg/dl and 12.3 mg/dl for virtual patients and 39.2 mg/dl and 36.6 mg/dl for virtual and real patients. These results confirm that linear models can be used as prediction models in model-based control strategies as predictive control.

INDEX TERMS Glucose dynamics, identifiability, practical identifiability, biomedical systems, model identification.

I. INTRODUCTION

Insulin and glucagon play a key role in glucose homeostasis. Insulin promotes glucose storage as glycogen and inhibits endogenous glucose production (EGP) while also promoting glucose utilization in insulin-dependent tissues. As a counterregulatory hormone, glucagon opposes to the action of insulin, actively stimulating hepatic glycogenolysis and gluconeogenesis and hence EGP to enhance a rapid rise in the systemic glucose concentration in postabsorptive and fasting periods, respectively. Unfortunately, the above is lost in Type 1 Diabetes (T1D). T1D is a chronic disease characterized by insulin deficiency due to the autoimmune

destruction of the pancreatic beta cells, leading to an alteration in the natural glucose regulatory system [1]. While T1D mainly affects endogenous insulin production, its absence (and even its exogenous administration) blunts the remaining glucose-related metabolic processes. In this regard, people with T1D face a lifelong optimization problem: limiting their exposure to hyperglycemia while simultaneously avoiding hypoglycemia [2]. Poorly controlled T1D increases the risk of short- and long-term complications such as diabetic ketoacidosis, retinopathy, nephropathy, and even death. [3].

Functional insulin therapy (FIT) deals with the accurate titration of both short and long-term multiple daily injections (MDI) of insulin as a function of daily glucose levels, pre-prandial glucose levels, and estimated carbohydrate (CHO) intake. According to the Diabetes Control and

The associate editor coordinating the review of this manuscript and approving it for publication was G. R. Sinha¹.

Complications Trial, FIT was related to a threefold increase in severe hypoglycemic risk [3]. Nevertheless, the benefits from transitioning the FIT from MDI to Sensor Augmented Pump (SAP) are widely recognized, reducing the variability of daily glucose profiles and the incidence of chronic complications [3]–[5].

A second treatment for T1D that is under continuous development is based on Artificial Pancreas Systems (APS). APS consist of a sensor-augmented insulin pump with a closed-loop control strategy to automatically titrate the patient's insulin infusion rate to keep blood glucose (BG) levels within safe limits. Model-based control strategies embedded into APS, such as Model Predictive Control (MPC), have gained considerable attention during the last decade [6]. MPC, rather than a single strategy, encompasses a flexible control paradigm including (i) an explicit mathematical model to predict the variable(s) of interest and (ii) an online optimization problem designed to find the best insulin injections subject to physical and design constraints over the model variables.

The so-called minimal models or control-oriented models target a simple mathematical description (few ordinary differential equations and parameters) to evaluate and optimize insulin therapies and design model-based control strategies, i.e., these models are usable for both closed-loop control in APS and open-loop control in FIT. The control-oriented models include black-box models developed from experimental data but are quite limited to properly represent the physiology of a patient [7], [8] and gray-box models based on physiological knowledge and real data [9]–[12]. Nevertheless, despite the number of models for T1D treatment, model individualization remains a challenge for three main reasons: (i) the error in CGM devices, (ii) the uncertainty linked to self-reported information from users (meal and exercise records, for instance) and (iii) physiological variations, such as the circadian rhythm, that affect the glucose regulatory system. Therefore, appropriate model individualization should be performed in order to minimize the overall model uncertainty. [13].

Model identification/individualization in diabetes technology deals with finding the model parameters that best describe the available data from a particular subject. The authors in [14] presented an identification method in which the glucose-insulin model is rewritten in terms of integrals to individualize the insulin sensitivity and the time-varying fractional clearance of plasma glucose at basal insulin. In [15], the linearized UVA/Padova model was individualized around a basal working point using a parametric identification technique driven by constrained optimization where the constraints are imposed over low and high glycemic values. A constrained optimization problem was also used in [16]–[18] where the sum of squared residuals was minimized to identify a minimal black-box model. This identification method was later improved in [19] by introducing a data-driven multiple-model predictor that uses three different identified models for specific periods of the day.

In [20], an adaptive identification procedure was provided by recomputing the parameters with every new measurement using a constrained weighted recursive least squares method with a time-varying forgetting factor λ . In [13], three minimal models were identified by minimizing the mean square error concerning the CGM measurements. In addition, a long-term glucose prediction algorithm based on a physiological model and a deconvolution technique using CGM data was presented in [21] by adding information about meal absorption to enhance prediction accuracy and using a constrained optimization technique that minimizes the mean absolute relative difference to identify 3 of the 10 parameters of the model.

In the context of T1D, other methods have been used as interval analysis where the uncertainties are considered with interval models by minimizing the sum of squares of the distance between the samples and the predicted envelope [22], [23]. Alternative identification strategies have also been proposed in other applications. For instance, to model prosthetic hand fingers, an online identification algorithm that uses Recursive Least Squares was implemented to identify the parameters of a Takagi-Sugeno-Kang fuzzy model [24], and a recurrent neural network was introduced in [25].

Although model individualization in the T1D field has been typically carried out informally [13], neglecting the lack of identifiability either in terms of the structure of the model (structural) or in terms of the quality of experiments/available data (practical) [26].

In this manuscript, a comprehensive review of control-oriented models for both hybrid and fully automated APS leveraging typical user-related physiological information is provided [10]. The review focuses on gray-box linear control-oriented models. Based on these models, four well-acknowledged linear models are analyzed in terms of structure, identifiability and observability, and their relationship with FIT. It is shown that most of these models are not fully identifiable and observable simultaneously, which implies that the parameters obtained in an overall identification procedure are not reliable. As a consequence of this analysis, the second contribution is the proposal of model structures that encompass the previous four linear models for the sake of information integration. Two minimal model structures are generated, which are globally identifiable and observable. Also, a discussion about practical identifiability is addressed, including a methodology to select portions of the data best suited for identification. This methodology is validated with the two model structures using data from 33 virtual subjects and 77 real subjects.

The paper is organized as follows. Section II provides a review of gray-box control-oriented models in the literature. In Section III, four linear control-oriented models [9]–[12] are analyzed and the structure of a general model is presented including their relationship with personalized tools for FIT. In Section IV, the identifiability and observability of all five models are analyzed. In Section V, the results are presented along with the collected data and the identification method used. In addition, long-term validation of the identified model

is carried out with in-silico and clinical data, the personalized tools for FIT are assessed, and the performance of open-loop control is also discussed. Finally, the conclusions are summarized in Section VII.

II. CONTROL-ORIENTED MODELS: A REVIEW

This section presents a chronological review of the control-oriented gray box models that stand out in the literature.

The introduction of the so-called glucose-insulin Minimal model (MM) is attributed to the pioneering work of Cobelli and Bergman at the end of the 1970s [27], [28], although earlier approaches to modeling the glucose homeostasis had already been acknowledged [29]. The term ‘minimal model’ was coined concerning the model’s level of complexity [30]. It is worth pointing out that, despite its importance in today’s diabetes technology, the model was initially intended to characterize the insulin sensitivity in health during an Intravenous Glucose Tolerance Test (IVGTT) instead of designing model-based control systems for T1D. This gray-box model is nonlinear, and composed of two separate parts: the first part describes glucose disappearance as a function of insulin in a remote compartment and consists of two ordinary differential equations. The second part consists of a single differential equation and describes plasma insulin concentration when BG concentration is a known forcing function. According to the authors, despite the model’s simplicity, it cannot be identified as a whole; this has to be done in two parts, which is generally not recommended.

In [31], the physiological nonlinear model known as Automated Insulin Dosage Advisor (AIDA) was introduced to describe glucose-insulin interaction in subjects with T1D. The model consists of four differential equations to account for the change of glucose concentration, the change of plasma insulin concentration, the ‘active’ insulin pool (which serve to describe the delay in insulin action), and the amount of glucose in the gut following the ingestion of a meal. With this model, glucose uptake is linear when insulin is varied at fixed glucose levels, but it saturates as glucose increases at fixed insulin. A comparison of Bergman’s MM, the AIDA, and the maximal model developed by [32] can be found in [33]. The comparison was performed only for the glucose/insulin subcomponent (glucose absorption due to meals was not considered) and included IVGTT in the absence and presence of an incremental change in insulin. Results showed that the three models accurately followed the BG profile in the presence of an incremental insulin response but failed to predict BG levels in the absence of insulin.

Other contributions followed and improved the line of Bergman’s MM. In [34], the authors analyzed previous linear compartmental and non-compartmental models for glucose kinetics in a steady state. The comparison revealed structural errors in the non-compartmental models, which make it difficult to obtain a physiological insight, especially when insulin is elevated. In contrast, despite being more demanding in terms of modeling and computational

effort, compartmental models allow for a better use of the informational content of kinetic data. In [35], [36], a non-linear two-compartment MM of glucose kinetics was introduced for labeled IVGTT. This model was required since the monocompartmental representation available at the time, provided a non-physiological pattern of hepatic glucose production. Thus, two glucose pools were used to describe glucose kinetics, one for plasma plus insulin-independent tissues and the other for insulin-dependent tissues slowly exchanging with plasma. This model was then improved in [37] to obtain a more reliable insulin-independent glucose disposal portrait and greater precision for metabolic indexes. The improved version of the two-compartment model relied on expressing insulin-independent glucose disposal as a fraction of steady-state glucose disposal instead of considering it as a constant. In addition, the authors in [38] added a model for the metabolism of glucose in the liver into the two-compartmental MM, to describe the endogenous glucose kinetics during IVGTT.

A large number of papers have dealt with modified versions of Bergman’s MM. The model proposed in [39] stands out as it introduces a simple delay-differential model to study glucose-insulin homeostasis as a single dynamical system. It eliminates the insulin remote compartment included in Bergman’s MM, and therefore, a single identification scheme is required, solving the previously described problem of the two-step identification scheme for Bergman’s MM. However, the model’s equilibria do not represent the reality of subjects with T1D because the basal rate depends on glycemia and stabilizes the system after a meal without an extra insulin injection. This last problem is not consistent with FIT and has appeared in many subsequent models. Models in [40]–[42] included a generalization of De Gaetano’s dynamical model and alternative ways of incorporating the time delay associated with the insulin action.

In [43], a modified MM for T1D was formulated by considering continuous insulin infusion, meals, and intravenous glucose administration (as in IVGTT) and with the feature of representing circadian insulin sensitivity. [44] also presented a model for T1D where Bergman’s MM was modified by replacing the endogenous insulin secretion with an exogenous insulin infusion. Also, an extended MM was formulated for the critically ill at the intensive care unit. Other works presenting models for glucose-insulin dynamics in critically ill patients are presented in [45]–[47] following the same basic structure of the MM. An extension of the MM to include plasma-free fatty acid dynamics with a primary focus on subjects with T1D was introduced in [48].

In [49], [50], a linear MM was presented and evaluated with data from subjects with T1D using a continuous subcutaneous insulin infusion (CSII). This model consists of two linear differential equations and represents the interaction of plasma glucose with insulin action. Although a rate of appearance of absorbed glucose is considered in the model, no dynamical model is added for the appearance of glucose due to meals. This linear model showed similar results to

Bergman's MM. In fact, it was shown that both models could not follow complex situations in T1D such as several insulin bolus injections, incorrect insulin dosage, or the absence of insulin supply. In [51], the Medtronic Virtual Patient model was presented. This nonlinear model consists of 5 equations that include three-compartment submodels coupled with Bergman's MM to describe plasma insulin concentration in response to subcutaneous insulin delivery and insulin effect, and a two-compartment model to describe glucose appearance following a meal based on the maximal model developed by Hovorka *et al.* [52], [53].

The last decade has seen tremendous progress on APS. This upswing can be attributed to advances in computer simulation, continuous glucose monitoring (CGM), insulin pumps, mobile platforms, and control systems. Regarding the latter, the analysis and development of control-oriented models of the glucose-insulin and glucose-insulin-glucagon systems have played a key role in model-based control strategies. In [54] and [55], a first-order with integrator and time delay continuous transfer function was proposed to account for the effect on BG of both, the CHO consumption and bolus insulin infusion. However, BG and insulin input are deviation variables around basal values. The model can be individualized with few FIT-related parameters. Following this idea, [9], [56]–[58] introduced a second-order with integrator transfer function to describe subjects under MDI. Even though initially the authors considered two different poles for each insulin and CHO subsystem, they observed that the BG behavior is similar when considering equal poles in each subsystem, so a reduced model was finally obtained with four parameters to be identified. In [59], a second-order transfer function plus a stochastic term was proposed to account for unknown factors not previously considered and useful for robust and adaptive control strategies.

In [60], the structural identifiability problem of Bergman's MM is discussed, which basically relies on fixing the basal glucose and insulin parameters to be identifiable. Thus, the authors presented an alternative identifiable nonlinear control-oriented model to describe plasma insulin action on glucose. The model consists of 3 Ordinary Differential Equations (ODE) and 4 parameters. In [61], a linear model with three state variables (insulin, glucagon, and glucose concentration) was developed. The control input is intravenous insulin, but despite the states' and inputs' physiological meaning, the parameters of the linear system have a non-physiological meaning. [62] extended the Bergman's MM to account for subcutaneous insulin infusion and meal intake based on Hovorka's model. Then, in [63], [64], the extended MM with meal absorption and CSII was also augmented with stochastic terms to include intra-patient variability. Additional works conducted up until 2013 can be seen in the review by [65]. In [66], two linear models were developed, and their steady-state response analyzed, arguing that the equilibrium of BG levels should depend on the initial BG condition. From this work, the linear model with improved BG predictions and parameter correlation with

therapy parameters has four parameters to identify as the one in [56]. Regarding bihormonal APS, Lv *et al.* proposed eight models including linear and nonlinear representations of the subcutaneous transport of exogenous glucagon [67], also in [68] a nonlinear control-oriented model including glucagon was detailed. A minimal model of 6 ODE introducing the effect of physical activity was presented in [69]. Additional models used up until 2015 can be seen in the review by [70].

In [10], a linear control-oriented model with close-to-reality equilibria and FIT-related parameters for subjects with T1D was presented. Its main feature consists of considering insulin sensitivity as a constant (i.e., not as a function of glucose) in the range of normoglycemia, hypoglycemia, and hyperglycemia. However, the insulin concentration and CHO absorption equations are given as second-order ODEs. In [71], a better state-space realization was performed where all variables have physiological meaning. The model was also analyzed and compared in terms of its identifiability property with a subcutaneous oral glucose MM and an intensive control insulin-nutrition-glucose model in [13]. The authors found that any of the three models are structurally identifiable. Several parameters must be fixed to fulfill this property.

Adopting a similar approach to [10], in [11], a linear glucose-insulin model with 3 sub-models (5 compartments) was developed. Based on the maximal model in [52], the authors got rid of one of the insulin compartments to avoid identifiability issues. In [72], 6 models were proposed (3 of them are linear) to characterize the influence of exogenous insulin on postprandial glucose kinetics. However, this time, the accessible compartments represented plasma, and the non-accessible compartments corresponded to other tissues such as the interstitium. Minimal physiological models similar to the Medtronic virtual patient [51] but extended with the model of CGM noise and stochastic terms to account for unknown factors were developed in [73], [74].

A brief review of physiological models, including some variants of the MM and Hovorka's model, was presented in [75], and a comprehensive review of different models including an analysis of 38 control-oriented models can be found in [76]. Another linear mathematical model was developed by [12] in order to simulate virtual patients for several days (19 days). The model included two-compartments for each subsystem of glucose, insulin, and CHO. A control-oriented linear parameter-varying model was developed in [77] consisting of a three-order transfer function, and then augmented to include the insulin-resistant effect of hyperinsulinemia in [78]. Also, a nonlinear model with four ODE to describe the interaction between insulin, glucose, free fatty acid, and growth hormone in T1D was introduced in [79].

III. MODEL STRUCTURE ANALYSIS

In the following section, we analyze some properties of control-oriented models that stand out because of their characteristics.

Bearing in mind that a good MM is not a large-scale one and has desirable features such as: (i) it is physiologically based, (ii) its parameters can be estimated with reasonable precision from a single dynamic response of the system, (iii) the parameters vary within physiologically plausible ranges, and (iv) the model has the ability to describe the dynamics of the system with the smallest number of identifiable parameters [30].

Additionally, as the overall nonlinearities of the dynamics of glucose in terms of insulin delivery and meal consumption have only a marginal effect [10], [50], [80], and as a linear structure is beneficial in the development of control strategies due to its simplicity, then the focus of this paper is on linear control-oriented models. From the state-of-art, four models are selected for satisfying these characteristics: Del Re’s model [56], Magdelaine’s model [10], Hovorka’s model [11], and Grosman’s model [12]. These models are discussed, and then a general model which summarizes their properties is proposed.

Each model’s structure is described in Table 1 along with their state-space representation. G denotes the BG concentration, I_1, I_2 are the insulin in the first and second compartment (interstice and blood), and D_1, D_2 denote the glucose concentration due to meals in the first and second compartment. The inputs of the models are the amount of ingested CHO $r(t)$ and the exogenous insulin delivered $u(t)$. A detailed description of the parameters and units of each model can be found in the corresponding reference.

A. LITERATURE MODELS

We start the analysis with the model presented in [56], denoted here as “Del Re’s model”, which, as stated by the authors, was intended for robust control design in MDI-treated subjects. The model comprises two transfer functions denoting the glucose response to a meal and an insulin injection, respectively. Table 1 shows the model’s realization, where only four parameters were used, implying, for instance, the time constant of insulin release being equivalent to the one needed for its degradation (a similar assumption is made for the meal dynamics).

We further consider the model presented in [10], denoted here as “Magdeleine’s model”. This is a simple model aimed at representing the realistic behaviors of a subject with T1D, focusing on the long term. The model describes BG excursions after meal intake while treated with insulin therapy. The model is made up of five state variables and six parameters. The main property of this model is that each glycemia equilibrium corresponds to a single value for the basal level, which is consistent with FIT because the basal level does not depend on the BG value. One of the model’s main features is that it keeps an unstable equilibrium in the fasting state, as observed in T1D. Unlike del Re’s model [56], this model includes the term $K_1 - K_b$ corresponding to endogenous glucose production and insulin-independent glucose consumption. Unlike many other linear/linearized models of the glucose-insulin system, the state variables in this model are absolute (no

deviation). Table 1 provides the block diagram and describing equations of the model.

The third model, denoted here as “Hovorka’s model,” is introduced in [11]. Its purpose is to produce realistic multi-day glycemic excursions of subjects with T1D with day-to-day variability in insulin therapy and meals. The inputs of the model are insulin dose and the amount of CHO intake. The model is made up of five compartments, and thus, five state variables. Unlike previous models, this model incorporates a glucose self-regulation parameter K associated with the renal clearance of glucose at high BG levels or counter-regulatory hormone effects at low BG levels, leading to glycemia stabilization. This is not consistent with the reality of patients with T1D because extra boluses of insulin would not be necessary after a meal; it would be enough to wait to self-regulate the levels. However, it can be justified if the constant K is small enough, implying a long stabilization time such that it cannot be reached during postprandial periods, so in this case, it is a model that is consistent with reality. Table 1 provides the block diagram and describing equations of the model.

Finally, the fourth model is presented in [12] and denoted as “Grosman’s model”. It is a mathematical model formulated to simulate virtual patients’ glucose dynamics derived from the information provided by the Medtronic MiniMed CareLink sensor-augmented pump during 19 simulation days. This linear model consists of three two-compartment submodels for glucose, insulin, and CHO dynamics, yielding a model of 6 states and 9 parameters. The model is very similar to the three previously described ones. As in Hovorka’s model, the self-regulation term $1/\tau_3$ has been included, and it considers equal poles for the meal absorption submodel. However, the model considers different poles for the insulin dynamics and has an additional state for subcutaneous BG concentration G_{sc} . The block diagram and describing equations of the model are provided in Table 1.

B. A GENERALIZED MODEL

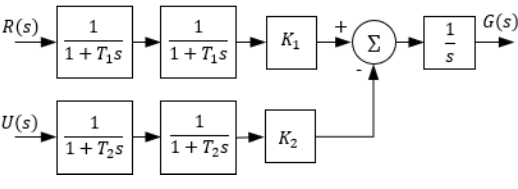
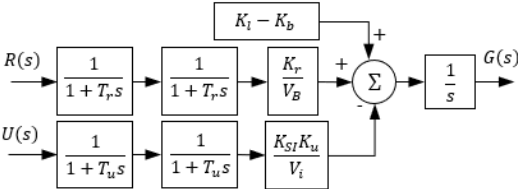
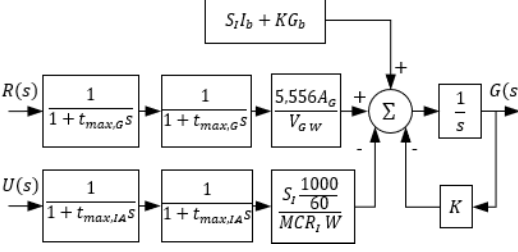
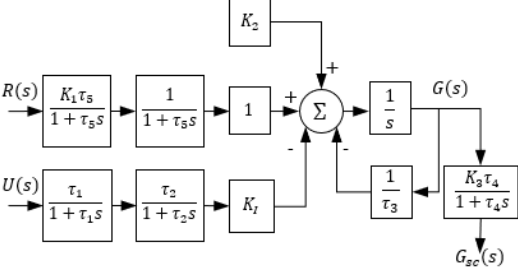
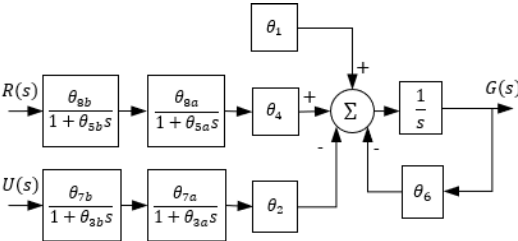
For the sake of simplicity, we present a generalization of the above models to condense the information and make the analysis easier. To this end, let us consider the following affine linear model with state-space representation

$$\begin{aligned} \dot{X}(t) &= AX(t) + BU(t) + E \\ Y(t) &= CX(t) \end{aligned} \tag{1}$$

with matrices given by:

$$A = \begin{bmatrix} -\theta_6 & -\theta_2 & 0 & \theta_4 & 0 \\ 0 & -1/\theta_{3a} & \theta_{7a}/\theta_{3a} & 0 & 0 \\ 0 & 0 & -1/\theta_{3b} & 0 & 0 \\ 0 & 0 & 0 & -1/\theta_{5a} & \theta_{8a}/\theta_{5a} \\ 0 & 0 & 0 & 0 & -1/\theta_{5b} \end{bmatrix},$$

TABLE 1. Structure of the models.

Model	Block diagram	ODEs
del Re [56]		$\dot{G}(t) = K_1 I_2(t) - K_2 D_2(t)$ $\dot{I}_2(t) = \frac{I_1(t)}{T_1} - \frac{I_2(t)}{T_1}$ $\dot{I}_1(t) = \frac{r(t)}{T_1} - \frac{I_1(t)}{T_1}$ $\dot{D}_2(t) = \frac{D_1(t)}{T_2} - \frac{D_2(t)}{T_2}$ $\dot{D}_1(t) = \frac{u(t)}{T_2} - \frac{D_1(t)}{T_2}$
Magdelaine [10]		$\dot{G}(t) = -K_{SI}I(t) + K_1 - K_b + D(t)$ $T_u^2 \frac{d^2 I(t)}{dt^2} + 2T_u \frac{dI(t)}{dt} + I(t) = \frac{K_u}{V_i} u(t)$ $T_r^2 \frac{d^2 D(t)}{dt^2} + 2T_r \frac{dD(t)}{dt} + D(t) = \frac{K_r}{V_b} r(t)$
Hovorka [11]		$\dot{G}(t) = -S_I(I(t) - I_b) + D(t) - K(G(t) - G_b)$ $\dot{I}_1(t) = -\frac{1}{t_{max,IA}} I_1(t) + \frac{u(t)}{60}$ $\dot{I}_2(t) = \frac{1}{t_{max,IA}} (I_1(t) - I_2(t))$ $I(t) = \frac{1000 I_2(t)}{t_{max,IA} MCR_I W}$ $\dot{D}_1(t) = -\frac{1}{t_{max,G}} D_1(t) + \delta t_j(t) r(t_j)$ $\dot{D}_2(t) = \frac{1}{t_{max,G}} (D_1(t) - D_2(t))$ $D(t) = \frac{5.556 A_G D_2(t)}{t_{max,G} V_G W}$
Grosman [12]		$\dot{G}_{sc}(t) = K_3 G(t) - \frac{1}{\tau_4} G_{sc}(t)$ $\dot{G}(t) = K_2 + D_2(t) - K_I I_2(t) - \frac{1}{\tau_3} G(t)$ $\dot{I}_2(t) = I_1(t) - \frac{1}{\tau_2} I_2(t)$ $\dot{I}_1(t) = u(t) - \frac{1}{\tau_1} I_1(t)$ $\dot{D}_2(t) = \frac{1}{\tau_5} D_1(t) - \frac{1}{\tau_5} D_2(t)$ $\dot{D}_1(t) = K_1 r(t) - \frac{1}{\tau_5} D_1(t)$
Generalized		$\dot{G}(t) = -\theta_6 G(t) - \theta_2 I_2(t) + \theta_4 D_2(t) + \theta_1$ $\dot{I}_2(t) = -\frac{1}{\theta_{3a}} I_2(t) + \frac{\theta_{7a}}{\theta_{3a}} I_1(t)$ $\dot{I}_1(t) = -\frac{1}{\theta_{3b}} I_2(t) + \frac{\theta_{7b}}{\theta_{3b}} u(t)$ $\dot{D}_2(t) = -\frac{1}{\theta_{5b}} D_2(t) + \frac{\theta_{8a}}{\theta_{5b}} D_1(t)$ $\dot{D}_1(t) = -\frac{1}{\theta_{5b}} D_2(t) + \frac{\theta_{8b}}{\theta_{5b}} r(t)$

$$B = \begin{bmatrix} 0 & 0 \\ 0 & 0 \\ \theta_{7b}/\theta_{3b} & 0 \\ 0 & 0 \\ 0 & \theta_{8b}/\theta_{5b} \end{bmatrix}, \quad E = \begin{bmatrix} \theta_1 \\ 0 \\ 0 \\ 0 \\ 0 \end{bmatrix}, \quad U(t) = \begin{bmatrix} u(t) \\ r(t) \end{bmatrix},$$

and $C = [1 \ 0 \ 0 \ 0 \ 0]$. The state is given by $X = [X_1, \dots, X_5]^T = [G \ I_2 \ I_1 \ D_2 \ D_1]^T$, and the inputs are insulin rate $u(t)$ and CHO intake rate $r(t)$. The ODEs of the model and the corresponding block diagram are shown in Table 1, where θ_1 is the net balance between the

TABLE 2. Relationships between model parameters.

Model	Parameters											
	Glucose subsystem				Insulin subsystem				Digestion subsystem			
General	θ_1	θ_2	θ_4	θ_6	θ_{3a}	θ_{3b}	θ_{7a}	θ_{7b}	θ_{5a}	θ_{5b}	θ_{8a}	θ_{8b}
Del Re	0	K_2	K_1	0	T_2	T_2	1	1	T_1	T_1	1	1
Magdelaine	$K_1 - K_b$	$\frac{K_{SI}K_u}{V_B}$	$\frac{K_r}{V_B}$	0	T_u	T_u	1	1	T_r	T_r	1	1
Hovorka	$S_I I_b + K G_b$	$\frac{S_I \frac{1000}{60}}{MCR_I W}$	$\frac{5.556 A_G}{V_G W}$	K	$t_{max,IA}$	$t_{max,IA}$	1	1	$t_{max,G}$	$t_{max,G}$	1	1
Grosman	K_2	K_I	1	$1/\tau_3$	τ_2	τ_1	τ_2	τ_1	τ_5	τ_5	1	$K_1 \tau_5$

endogenous glucose production and insulin independent glucose consumption, θ_2 is the insulin sensitivity, θ_{3a} and θ_{3b} correspond to the time constants of insulin diffusion in the first and second compartment, respectively, θ_4 is the conversion constant of CHO to glycemia, θ_{5a} and θ_{5b} are the time constants of CHO diffusion in the first and second compartment, respectively, θ_6 is the glucose self-regulation fractional rate, θ_{7a} and θ_{7b} are the insulin bioavailability in the first and second compartment, and θ_{8a} and θ_{8b} are the CHO bioavailability in the first and second compartment.

This representation summarizes the previous models and adds some degrees of freedom by considering different time and bioavailability constants for each compartment. The relations between the original parameters of the analyzed models with respect to the new ones are shown in Table 2.

C. FUNCTIONAL INSULIN THERAPY

FIT is a pedagogical approach to insulin therapy for subjects with T1D. It empowers the patient to take control of the treatment based on his/her clinical history, lifestyle, diet, and everyday activities [81]. FIT involves frequent self-monitoring of blood glucose (6 to 8 daily controls), multiple daily insulin injections, and the subject’s therapeutic and nutritional education. The main FIT parameters are the basal insulin infusion rate (u_b) and the fast-acting insulin (bolus), which further depend on correction factor (CF), raise, carbohydrate-to-insulin ratio (CIR), and insulin-on-board (IOB). These tools are usually empirically calculated by the physician using a population approximation (see [82]), which involves a long process to obtain the specific value for a subject [83]. One of the purposes of mathematical models for T1D treatment along with the subject’s data and computation tools is to estimate subject-specific tools for FIT. These tools can be computed with the general model’s parameters, and therefore, with the other four models’ parameters by using the equivalences in Table 2. The description of each tool for FIT and its mathematical expression are presented in Table 3.

IV. STRUCTURAL IDENTIFIABILITY AND OBSERVABILITY

The purpose of an identification process is to provide a value for every parameter such that the model accurately describes the data collected for a given user. To this end, the model’s identifiability and observability are analyzed first. Identifiability can be seen as a particular observability

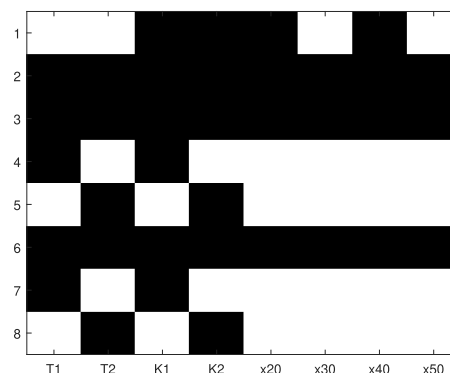


FIGURE 1. Reduced identifiability tableau - Del Re’s model.

case, in which the initial states are considered model parameters, thus, a system is defined identifiable if all its parameters are observable [84].

Structural identifiability refers to the theoretical possibility to find a unique solution (set of parameters θ) in the identification problem, where confidence intervals are not infinite [85]. It is a property of the model and cannot be improved through measurements since it does not depend on them.

Different methods and tools assessing structural identifiability can be found in [86], [87]. In this work, the Generating Series for Testing Structural Identifiability (GenSSI) tool was used for structural identifiability analysis, which relies on identifiability tableaus to determine whether the property is local or global. The tableaus graphically represent the fulfillment of the conditions of structural identifiability. They have as many rows as nonzero coefficients and as many columns as parameters to identify. When the tableau is a full-rank matrix, at least local identifiability is guaranteed.

A. LITERATURE MODELS

Figures 1, 2, 3, and 4 show the reduced tableaus of the four analyzed models when considering the complete set of parameters and initial conditions. A summary of the outcomes is shown in Table 4. Results show that the only globally structurally identifiable and simultaneously observable model is Del Re’s because its reduced identifiability tableau

TABLE 3. Relationship of the general model with tools for FIT.

Tool for FIT	Description	Equation
Basal Insulin (u_b)	Constant insulin infusion rate required to maintain glycemia at a target G_{Tar} during fasting.	$u_b = \frac{\theta_1}{\theta_2\theta_{7a}\theta_{7b}} - \frac{\theta_6}{\theta_2\theta_{7a}\theta_{7b}}G_{Tar}$
Correction Factor (CF)	Also known as insulin sensitivity. It represents the glycemic drop per unit of insulin (IU) when the basal insulin is correctly set.	$CF = \theta_2\theta_{7a}\theta_{7b}$
Raise (RF)	Represents the increase of BG levels due to the action of 1g of CHO, when the basal insulin is correctly set.	$RF = \theta_4\theta_{8a}\theta_{8b}$
Insulin to CHO ratio (CIR)	Represents the amount of grams of CHO that compensate for a unit of insulin (IU), when the basal is correctly set.	$CIR = \frac{CF}{RF}$
Insulin on Board (IOB)	Remaining insulin in the blood, due to the last insulin injection applied.	$IOB(t) = \frac{\theta_2\theta_{7a}\theta_{7b}}{\theta_{3a} - \theta_{3b}} (e^{-t/\theta_{3a}} - e^{-t/\theta_{3b}}) U_0$ $IOB(t) = \frac{\theta_2\theta_{7a}\theta_{7b}}{\theta_{3a}^2} t e^{-t/\theta_{3a}} U_0, \text{ if } \theta_{3a} = \theta_{3b}$
Bolus calculator	Insulin infusion rate recommended to compensate for meal intake and deviations to target G_{Tar} .	$u_{bolus}(t) = \frac{G(t) - G_{Tar}}{CF} + \frac{g_{CHO}}{CIR} - IOB(t)$

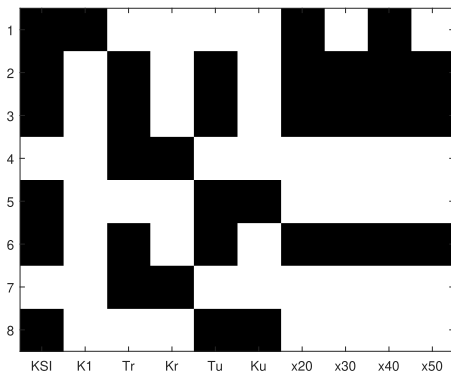


FIGURE 2. Reduced identifiability tableau - Magdelaine's model.

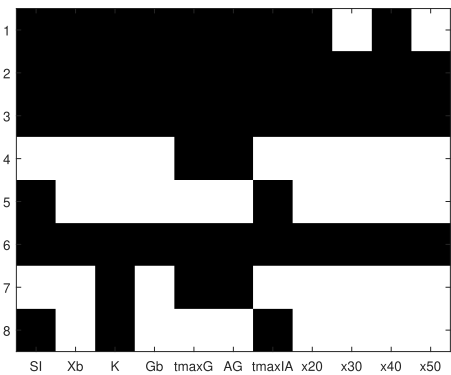


FIGURE 3. Reduced identifiability tableau - Hovorka's model.

is a full-rank matrix of order 8. This may be explained by the low number of parameters. However, simpler models tend to overlook important phenomena. Hovorka's, Magdelaine's, and Grosman's models do not satisfy the global identifiable and observable (GIO) condition when only considering the CGM data as output and the CHO intake and insulin doses as input signals. The lack of identifiability can be explained by

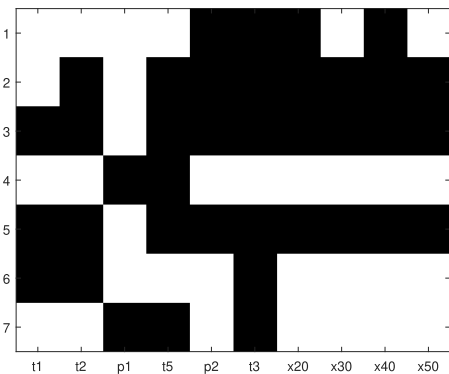


FIGURE 4. Reduced identifiability tableau - Grosman's model.

TABLE 4. Summary of literature models structure: BA-Bioavailability; EP-Equal poles; SR-Self-regulation; LI-Locally identifiable; GI-Globally identifiable; GIO-Globally identifiable and observable; NU-Number of unknown parameters.

Model	BA ≠ 1	EP	SR	LI	GI	GIO	NU	Ref.
Del Re	X	✓	X	✓	✓	✓	4	[56]
Magdelaine	X	✓	X	X	X	X	6	[10]
Hovorka	X	✓	✓	X	X	X	7	[11]
Grosman	X	✓	✓	✓	X	X	7	[12]

correlated parameters and ambiguous solutions which make it impossible to find a unique set of parameters.

B. GENERAL MODEL

In an initial analysis, it was shown that the complete parameter set, including the initial conditions of the state

$$\theta = [\theta_1, \dots, \theta_8, X(0)]^T$$

is not globally structurally identifiable (although local structural identifiability holds). Different combinations of parameters were assessed in terms of structural identifiability, considering different bioavailability rates, equal poles in both subsystems, and the self-regulation term, to find minimal realizations that are both globally identifiable and

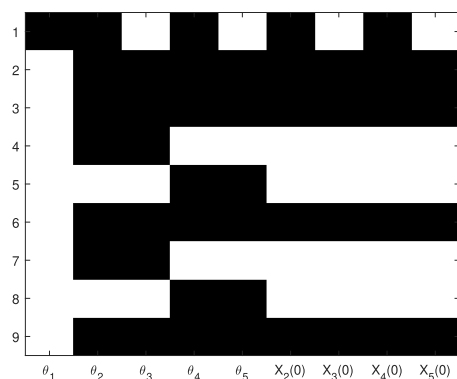


FIGURE 5. Reduced identifiability tableau - 5θ model (Str. A).

TABLE 5. Summary of general model structure variations: BA–Bioavailability; EP–Equal poles; SR–Self-regulation; LI–Locally identifiable; GI–Globally identifiable; GIO–Globally identifiable and observable; NU–Number of unknown parameters.

Model	BA ≠ 1	EP	SR	LI	GI	GIO	NU
12θ (General)	✓	✗	✓	✓	✗	✗	12
11θ	✓	✗	✗	✓	✗	✗	11
10θ	✓	✓	✓	✓	✗	✗	10
9θ	✓	✓	✗	✓	✗	✗	9
8θ	✗	✗	✓	✓	✗	✗	8
7θ	✗	✗	✗	✓	✗	✗	7
6θ (Structure B)	✗	✓	✓	✓	✓	✗	6
5θ (Structure A)	✗	✓	✗	✓	✓	✓	5

observable. The tested variations of the general model are detailed in Table 5, in which a reduction of parameters was made until a structure was found to be GIO. Two of these variations are further analyzed.

1) STRUCTURE A

This structure simplifies the general model as follows: $\{\theta_{7a}, \theta_{7b}, \theta_{8a}, \theta_{8b}\} = 1$, $\{\theta_{3a}, \theta_{3b}\} = \theta_3$, and $\{\theta_{5a}, \theta_{5b}\} = \theta_5 = \theta_6 = 0$ i.e., all bioavailability parameters are set as 1, the time constants are equal for each insulin and oral subsystem, and the self-regulation term is not considered. With this modification, the 4 initial states are deemed identifiable (the glycemia value is known as it is the output signal) together with the 5 resulting model parameters. The structure is similar to Magdelaine’s model, but provides a solution to the ambiguity problem generated by the parameters K_{SI} and K_u by grouping both into $\theta_2 = K_{SI}K_u/V_i$. This minimal realization yield both subsystems with critically damped dynamics.

Figure 5 shows the tableau for the general model with structure A. We can see that the matrix is full-rank of order 9; therefore, the model satisfies the condition of structural identifiability.

2) STRUCTURE B

This structure extends structure A with the self-regulation term θ_6 . Fasting conditions for the initial state are considered. The initial condition states $X_2(0)$ and $X_3(0)$ are set in

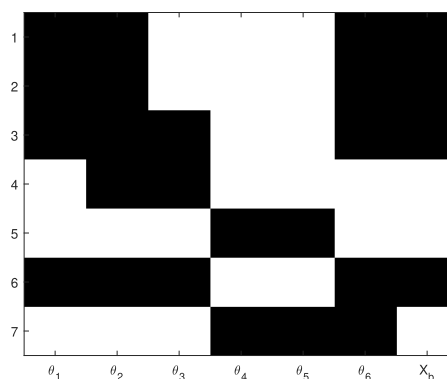


FIGURE 6. Reduced identifiability tableau - 6θ model (Str. B).

equilibrium X_b associated to the basal infusion rate, and $X_4(0)$ and $X_5(0)$ are set as zero due to the absence of boluses. The above holds only after several hours with no meal intake nor insulin bolus, i.e., in the steady-state. With the above, the model with structure B becomes GI and partially observable.

Figure 6 shows the full-rank tableau for the generic model with structure B. Although this structure has more parameters in the model, structure A has a constraint-free initial state.

V. PRACTICAL IDENTIFIABILITY

Once the structural identifiability of the model is studied, the next step is to perform a practical identifiability analysis to determine whether it is possible to find a unique numerical solution from noisy measurements, in this case, CGM data. In terms of model individualization, experimental design poses a significant challenge in diabetes technology since a persistent exciting signal cannot be directly applied to a real subject. Therefore, the model must be identified with input-output data collected in outpatient conditions. The output of the system is the data received by the CGM device corresponding to the glycemia measurements every 5 minutes. The first input corresponds to the delivered insulin doses. For this input, both the basal insulin and the insulin boluses are taken into account. Typically, the basal application is programmed into the insulin pump, while the boluses are calculated by the patient at mealtimes (keeping it as a record in the insulin pump memory). The second input corresponds to the CHO count made by the user at mealtime and reported either in the insulin pump or the CGM application. The most significant error source for the identification process comes from the last two entries, as it depends entirely on the patient’s report.

Non-identifiable parameters can often be approximated to fixed (population) values as long as their influence on the measured variable is not significant. In this regard, modeling strategies should target parameter identifiability for the most influential parameters. As presented in [13], [26], parameters can be ranked in terms of an importance factor, e.g., the individual sensitivities of the measured variable to changes in a given parameter set.

First, let us consider the matrix that includes the sensitivity terms of the output with respect to the model parameters

$$S = \frac{\partial Y(t)}{\partial \theta} = [S_{\theta_1} \quad \dots \quad S_{\theta_n}] = \begin{bmatrix} \frac{\partial Y_1}{\partial \theta_1} & \dots & \frac{\partial Y_1}{\partial \theta_n} \\ \vdots & \ddots & \vdots \\ \frac{\partial Y_k}{\partial \theta_1} & \dots & \frac{\partial Y_k}{\partial \theta_n} \end{bmatrix} \quad (2)$$

where $S_{\theta_1} \dots S_{\theta_n}$ can be computed by expanding system (1) with the sensitivity S_{θ_i} as a new state with initial conditions equal to zero. The sensitivity matrix can be computed through the Advanced Model Identification using Global Optimization (AMIGO) software [26] along with the importance factor (3) which will be helpful to rank the parameters.

To consider a sensitivity analysis valid for the entire space, n_{lhs} different parameter sets within the possible range are found using the Latin Hypercube Sampling (LHS) method [88]. The importance factor for each parameter is given by

$$\delta_{\theta_i}^{msqr} = \frac{1}{n_{lhs} k} \sqrt{\sum_{l=1}^{n_{lhs}} \sum_{e=1}^{n_e} (S_{\theta_i}^{l,e})^2} \quad (3)$$

where n_e refers to the number of experiments. The higher the factor for a particular parameter, the more relevant the effect of the parameter on the output. Thus, for non-identifiable models, this method is commonly used to consider only the most relevant parameters and set the parameters to be less sensitive to population values [13]. To guarantee uniqueness in the solution, linear independence between/among columns of the relative sensitivity \hat{S} matrix should be verified

$$\hat{S} = \begin{bmatrix} \frac{S_{\theta_1}}{\|S_{\theta_1}\|} & \dots & \frac{S_{\theta_n}}{\|S_{\theta_n}\|} \end{bmatrix} \quad (4)$$

There are several methods to determine the collinearity degree in a group of parameters. The collinearity index [89] $C_D(\theta)$ is used here to quantify that correlation

$$C_D(\theta) = \frac{1}{\sqrt{\lambda_{\hat{S}^T \hat{S}}}}, \quad (5)$$

with $\lambda_{\hat{S}}$ the minimum eigenvalue of the sensitivity matrix relative to $\hat{S}^T \hat{S}$. This index indicates that a change in the output Y caused by a variation of parameter θ_i can be compensated in a linear approximation of up to $1/C_D\%$ with appropriate changes in the other parameters. In [89], a C_D boundary of 20 was proposed. This means that the change in Y can be compensated by up to $1/20 = 5\%$ of changes in the other parameters. A high value of C_D indicates that the parameter set is weakly identifiable with the collected data, while low values suggest linear independence of the parameter set.

Collinearity tests in virtual and real subjects with T1D were performed at different time intervals. Using the sensitivity analysis in the collected data and for structures A and B, the collinearity index was evaluated in periods of 3 hours from the start of the data up to 5 days. The results obtained are shown in Figures 7-10. On average, the minimum collinearity

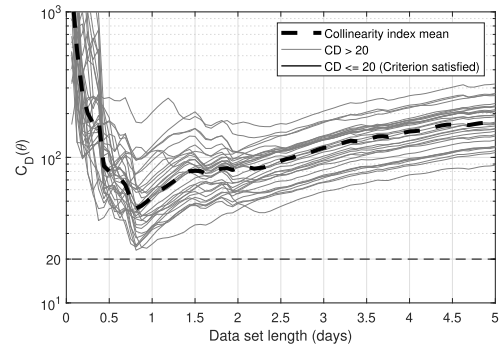


FIGURE 7. Collinearity index C_D - Virtual patients, Str. A.

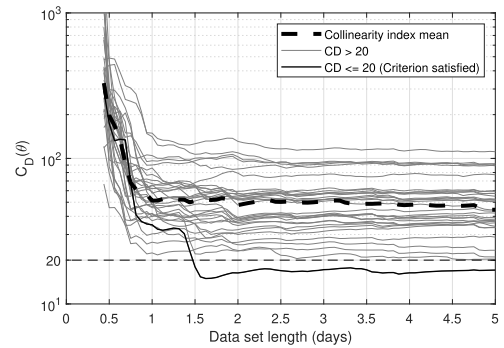


FIGURE 8. Collinearity index C_D - Virtual patients, Str. B.

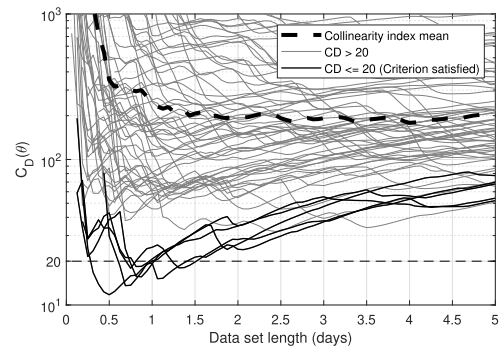


FIGURE 9. Collinearity index C_D - Real patients, Str. A.

index was reached in around one and a half days. This could be explained by the input pattern since insulin and mealtimes do not vary too much from day to day. Thus, longer periods usually have the same distribution, and the collinearity index remains constant or increases as denoted in Figures 7-10.

Due to a large amount of data in real subjects, it was necessary to find the time interval that minimizes the collinearity index and improves practical identifiability. A genetic algorithm to craft identification data sets minimizing the collinearity degree among parameters was implemented to achieve this. For Structure B, the initial time was restricted to periods between 3 am to 6 am, in an attempt to guarantee that all states are steady.

Initial parameters are necessary to minimize the C_D , which were estimated considering an initial interval of 2 days. A lower collinearity index was then found for every real patient by varying the interval using a genetic algorithm.

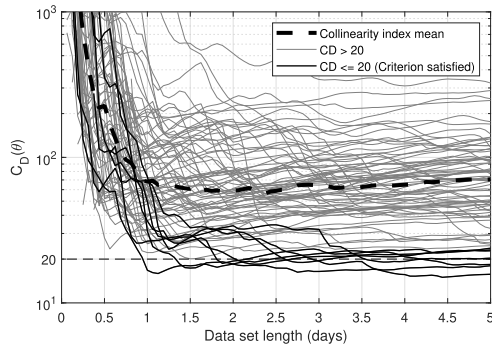


FIGURE 10. Collinearity index C_D - Real patients, Str. B.

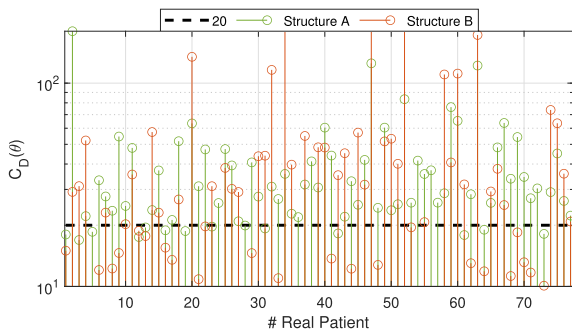


FIGURE 11. Collinearity index C_D - Real patients, optimal index.

Figure 11 shows the collinearity index (C_D) obtained for each patient and for structures A and B, where 14 and 33 intervals satisfy the condition $C_D \leq 20$, respectively, in comparison to the C_D previously reported in figures 9 and 10, where only 5 and 7 intervals satisfied this condition. The median of the collinearity index was 28.7 for Structure A and 25.2 for Structure B. This outcome may be due to the strong correlation between inputs (a bolus accompanies meals in most cases) and because of the almost invariant pattern of basal levels from day to day.

VI. IDENTIFICATION AND VALIDATION

In this section, the two model structures A and B are identified with the suitable data sets defined in the practical identifiability analysis, and the validation of each model for the virtual and real subjects is presented. Figure 12 shows an overview of the whole process required for model identification.

The first step for identification is the discretization of the models since the CGM measurements are obtained with a sampling time of $t_s = 5$ min. Here, a zero-order holder and sampler is considered, yielding

$$\begin{aligned} x(k) &= A_d x(k-1) + B_d \begin{bmatrix} u_i(k-1) \\ u_m(k-1) \\ u_f(k-1) \end{bmatrix}, \\ y(k) &= C_d x(k), \end{aligned} \quad (6)$$

where $y(k)$, $u_i(k)$, $u_m(k)$, and $x(k)$ represent the output, insulin injection, CHO amount, and state at the k -th sample. The fictitious input $u_f(k-1)$ is set to 1, and B_d is the discrete

Guidelines to perform the identification of a model

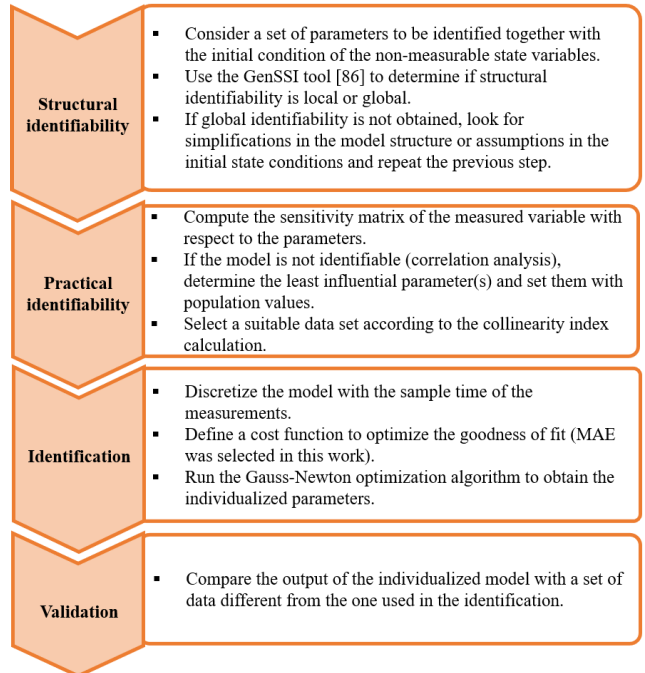


FIGURE 12. Guidelines to perform the identification of a model.

equivalent of the augmented matrix $B_d = [B E]_d$. The input u_m (derived from the meal announcement) is a variable duration pulse constructed as follows: $u_m = \bar{u}_m$ during $n = \lfloor (g_{CHO}/T_s)/\bar{u}_m \rfloor$ steps, where g_{CHO} [g] is the CHO amount, and $u_m = (g_{CHO}/T_s - n\bar{u}_m) \geq 0$ in the next step. The upper bound of u_m is empirically set to $\bar{u}_m = 2$ [g/min]. However, it should be an average physiological parameter that depends on the body mass index.

Following this, the identification problem is posed as an optimization problem such that the error between the data collected from the subject with T1D and the individualized model is minimized. As per usual, the mean square error function (MSE) is chosen as the cost function, which reads as

$$\text{MSE} = f(\theta) = \frac{1}{m} \sum_{k=0}^m (Y[k] - y[k, \theta])^2, \quad (7)$$

where $y(k, \theta)$ represents the model output and $Y(k)$ the actual measurement of the system at time k . The performance index is defined as the mean absolute error (MAE) to explain the model error in mg/dL units. This function range is between 0 and ∞ mg/dl, indicating an ideal and poor fit, respectively.

In this application, the system does not use persistent excitation (neither insulin doses nor carbohydrate content can be persistently varied in a real subject). Therefore, the identification procedure should be performed using historical records of CGM, meal, and insulin uploaded from the user devices. In this regard, a gradient-based optimization technique is

suitable for the identification procedure. Thus, the iterative Gauss-Newton algorithm is used here to individualize the proposed model [90] as shown in Algorithm 1.

Algorithm 1 Gauss-Newton

```

1: Define  $\theta[0]$  {Initial parameters and states}
2: while  $\max(\text{dir}) \geq \text{ToI}_{dir}$  &  $k \leq \text{Lim}_k$  do
3:    $\alpha \leftarrow 1$  {Initial step size}
4:    $\text{dir} \leftarrow -H_f(\theta)/J_f(\theta)$  {Max. slope}
5:    $i \leftarrow 0$ 
6:   while  $f[i] \geq f[i - 1]$  &  $f_c \leq \text{Lim}_{f_c}$  do
7:      $\theta[i + 1] \leftarrow \theta[i] - \alpha \text{dir}$  {Parameters update}
8:     Calculate  $f(\theta)$ ,  $J_f(\theta)$  y  $H_f(\theta)$ 
9:      $f_c \leftarrow f_c + 1$ 
10:     $\alpha \leftarrow \alpha/2$  {Step size update}
11:  end while
12:   $i \leftarrow i + 1$ 
13: end while
14: return  $\theta$  {Final guess of parameters} = 0
  
```

The algorithm finds the parameters θ that minimize the MSE in (7), and computes the step direction as $\frac{H_f(\theta)}{J_f(\theta)}$, where $J_f(\theta)$ and $H_f(\theta)$ are the Jacobian and Hessian of function f with respect to θ , which are given by:

$$J_f(\theta) = \frac{\partial f}{\partial \theta} = \frac{2}{m} \sum_{k=0}^m (Y[k] - y[k, \theta]) J_Y(\theta), \quad (8)$$

$$H_f(\theta) = \frac{\partial J_f(\theta)}{\partial \theta} \approx \frac{2}{m} \sum_{k=0}^m J_Y(\theta) J_Y^T(\theta), \quad (9)$$

$$J_Y(\theta) = C_d \frac{\partial x}{\partial \theta} = C_d \begin{bmatrix} \frac{\partial x_1}{\partial \theta_1} & \dots & \frac{\partial x_1}{\partial \theta_n} \\ \vdots & \ddots & \vdots \\ \frac{\partial x_5}{\partial \theta_1} & \dots & \frac{\partial x_5}{\partial \theta_n} \end{bmatrix}, \quad (10)$$

Finally, the parameters are computed as:

$$\theta[i + 1] = \theta[i] + \alpha \frac{H_f(\theta)}{J_f(\theta)}, \quad (11)$$

in which the step α is initialized as 1, and the parameters are initialized with $\theta(0) = [u_b ISF, ISF, 80, ISF/CR, 50, 0.005]$ (θ_6 only applies for Structure B), where the constant values are population parameters extracted from the literature. The initial state is taken during the fasting period (no meal consumption) considering a fixed insulin infusion equal to the basal value (i.e., $x_2(0) = x_3(0) = u_b$, $x_4(0) = x_5(0) = 0$). The error curve of this method (descending gradient type) has several local minimums. Therefore, convergence to the global minimum is achieved when the initial value of the parameters vector θ is closer to the global minimum than to another neighboring local minimum. Matlab was used to perform the whole procedure. The calibration (identification) dataset is the one defined by the collinearity index that minimizes the input correlation metric.

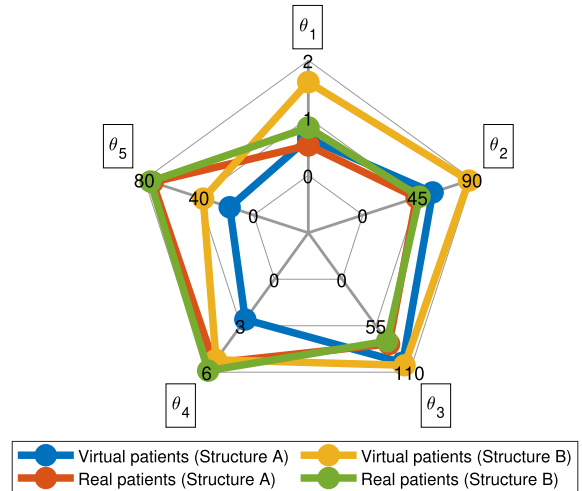


FIGURE 13. Parameter comparison between structures A and B in virtual and real subjects.

Structures A and B were identified during fixed periods of 3 days in virtual subjects and variable periods in real subjects (depending on the interval with the lowest collinearity index). Next, the individualized model is validated by comparing the output of the model with data compiled during the 24-hours following the calibration period for both virtual and real subjects.

The data for 33 virtual subjects was obtained from the UVA/Padova simulator. A simulation scenario was created in which five different basal segments were applied each day. For the identification period the input of meals was defined as [(32, 5, 67, 20, 42), (52, 27, 67, 39, 51), (37, 11, 69, 17, 42)], and for the validation period as [(45, 15, 85, 54)] grams of CHO. An insulin bolus was delivered for each meal, whose amount was suggested by the UVA/Padova simulator bolus calculator [91]. On the other hand, the data relating to 77 real adult subjects with T1D were collected from 2017 to 2019 (Clinica Integral de Diabetes, Medellin, Colombia). The hardware configuration used for data collection was the Paradigm Veo System, composed of CGM and an insulin pump. Four models of pumps were found: Minimed Paradigm 722, 723, 754, and 640G, which have recently been updated with the current model 670G. All the identification scripts and data can be found at <https://github.com/judhoyosgi96/DM1-script>.

The identification results using the Gauss-Newton method are reported in Table 6, which presents the parameters, initial states, the adjustment in the periods of identification (MAE_{id}) and validation (MAE_{val}), and tools for FIT, where the sub-index “real” indicates the population value calculated by the UVA/Padova simulator (for virtual subjects) or the one reported in the insulin pump (for real subjects). Finally, the metric denoted as RE_z indicates the relative error between the real value and the identified value of variable z .

TABLE 6. Summary of identified parameters, initial states, and FIT tools using structures A and B.

Symbol	Structure A		Structure B	
	Virtual	Real	Virtual	Real
θ_1 [mg/dl/min]	0.6449 ± 0.3171	0.5231 ± 0.3611	1.6227(1.6003)	0.8316(1.2412)
θ_2 [mg/dl/U]	57.4 ± 34.8	44.1 ± 23.8	87.3(115.5)	46.6(30.1)
θ_3 [min]	98.7 ± 38.9	76.6(84.3)	101.8 ± 48.9	73.3(53.8)
θ_4 [mg/dl/gCHO]	2.6 ± 0.8	5.4(4.5)	5.2(4.1)	5.9(6.2)
θ_5 [min]	17.6 ± 3.4	74.0(68.4)	37.0(12.1)	75.6 ± 57.1
θ_6 [min ⁻¹]	N.A.	N.A.	0.0060(0.0076)	0.0014(0.0067)
$X_2(0)$ [U] X_b [U]	0.019(0.029)	0.465(1.745)	0.013 ± 0.008	0.009(0.017)
$X_3(0)$ [U]	0.023 ± 0.014	0.160(0.454)	N.A.	N.A.
$X_4(0)$ [gCHO]	0.295 ± 0.360	4.071(13.533)	N.A.	N.A.
$X_5(0)$ [gCHO]	0.487(0.912)	1.737(4.716)	N.A.	N.A.
MAE_{id} [mg/dl]	16.8 ± 4.2	21.6 ± 7.0	9.9 ± 1.8	21.5 ± 7.4
MAE_{val} [mg/dl]	23.9 ± 9.7	39.2 (31.8)	12.3 ± 3.2	36.6 (32.9)
$u_{b_{real}}$ [U/h]	0.841 ± 0.414	0.651 ± 0.312	0.841 ± 0.414	0.648 ± 0.308
u_b [U/h]	0.842 ± 0.419	0.747 ± 0.395	0.921 ± 0.456	0.944 ± 0.565
RE_{u_b} [%]	5.4 ± 4.3	25.6 (47.4)	10.1 ± 8.3	39.4 (67.6)
CIR_{real}	20.0 ± 7.2	8.9 ± 4.8	20.0 ± 7.2	7.6 (5.6)
CIR [gCHO/U]	20.6 ± 7.9	7.4 (5.4)	16.7 ± 6.1	8.5 ± 4.9
$RECIR$ [%]	9.4 ± 5.5	17.3 (27.3)	15.6 ± 12.8	29.8 ± 21.9
CF_{real} [mg/dl/U]	72.4 ± 37.7	57.3 ± 16.9	72.4 ± 37.7	57.3 ± 16.7
CF [mg/dl/U]	57.4 ± 34.8	44.1 ± 23.8	87.3 (115.5)	46.6 (30.1)
REC_F [%]	31.4 ± 17.8	37.6 ± 24.9	35.0 (95.4)	28.8 (30.6)

Outcome metrics are reported as Mean ± SD for normally distributed data and as median (IQR) otherwise.

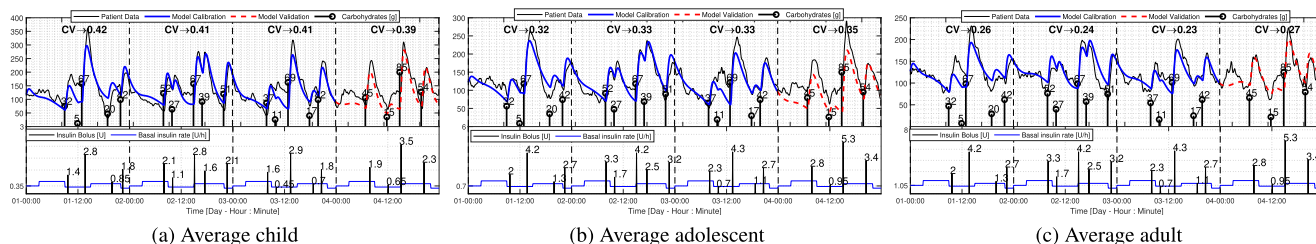


FIGURE 14. Model fit of virtual patients - 5θ model (Structure A).

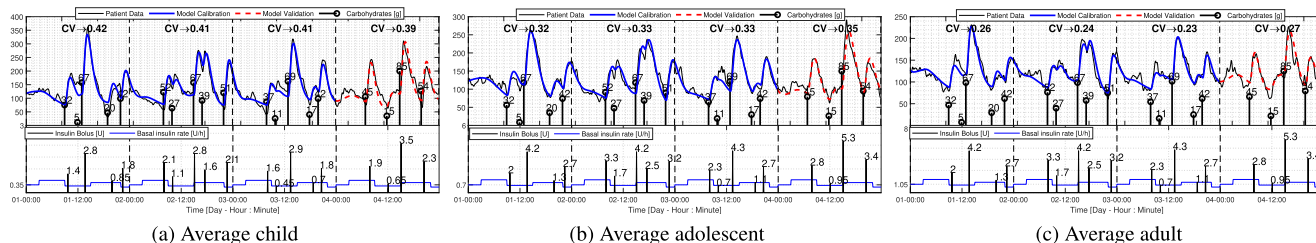


FIGURE 15. Model fit of virtual patients - 6θ model (Structure B).

The outcomes are reported as mean ± standard deviation for normally distributed data and as median (interquartile range) otherwise.

A better fit to the curve in virtual subjects was obtained with Structure B than Structure A. However, with Structure B, the results in terms of FIT tools are not improved when comparing them to nominal values in UVA/Padova simulator. On the other hand, the fit to the curve was not improved for real subjects when using Structure B. We can speculate that this is due to more significant variability in the real subjects than the virtual subjects.

Figure 13 shows the comparison of structures A and B, with data of virtual and real subjects. Although all parameters are close on every scenario, time constants θ_4 and θ_5 are bigger in real patients than they are in virtual ones under both structures. This could be explained by the uncertainty of the (self-reported) meal record.

Figures 14 and 15 show the model fit on the average virtual subjects (child, adolescent, and adult) of the UVA/Padova simulator when using structures A and B in the identification and validation periods. An improvement in MAE can be seen when using Structure B ($MAE_{id} = 9.9$ mg/dl,

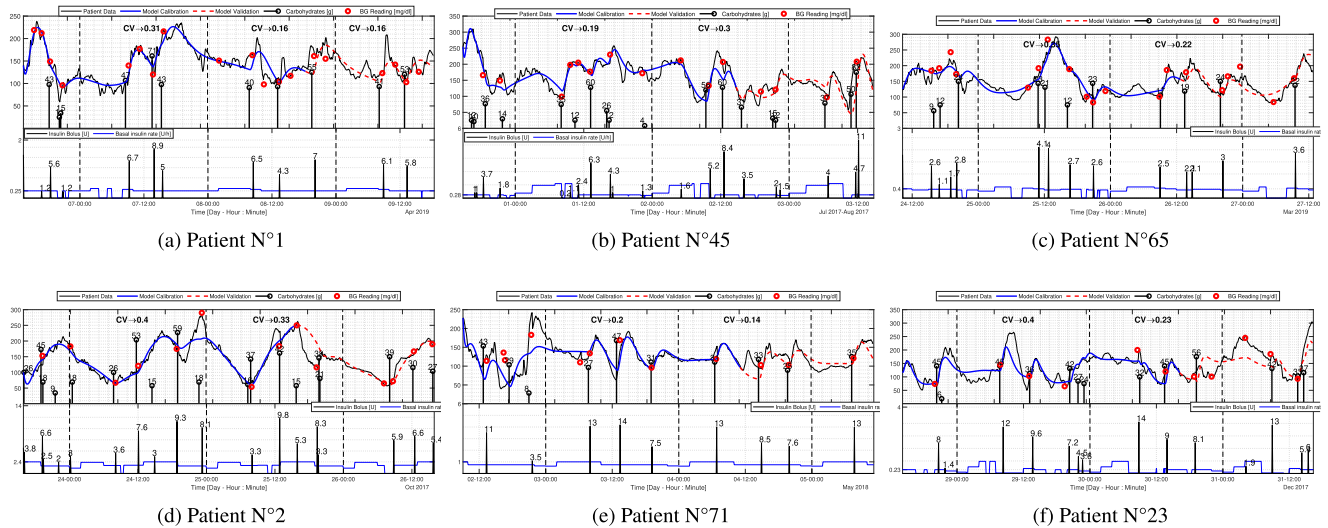


FIGURE 16. Model fit of real patients - 5th model (Structure A).

$MAE_{val} = 12.3$ mg/dl) with respect to Structure A ($MAE_{id} = 16.8$ mg/dl, $MAE_{val} = 23.9$ mg/dl).

Figure 16 shows the model fit after identifying Structure A with data for real subjects. The identification period was defined according to the collinearity index (an average interval duration of 2 days was obtained). For Structure A, 6 subjects are depicted with satisfactory results, representing the glycemic dynamics within both the calibration and validation periods. Complete results are shown in the Table 6 for structures A and B. Poor performance can sometimes be explained by inaccurate data, i.e., data sets with missing CHO or bolus entries, intra-patient variability, and non-accounted non-linear behavior.

VII. CONCLUSION

Model-based APS use a prediction model of the glucose-insulin system to plan timely insulin therapy. Linear control-oriented models can provide acceptable prediction accuracy while keeping the computational load stable. To guarantee the uniqueness of the solution after the identification process, an analysis of structural and practical identifiability is required. In this work, four linear models of the literature were studied, and a general model was proposed that summarizes the dynamics described in all of them. Using different parameter combinations, two minimal globally and structurally identifiable realizations were proposed, which were identified with simulated and real data. Satisfactory results were obtained in both data sets, fitting the CGM measurements and estimating the tools for FIT. Although Structure A better represents glycemic behavior in subjects with T1D, Structure B can be useful in some cases, as evinced in virtual patients. These structures also allow patients’ individualization and, through a practical identifiability analysis, the definition of reliable data chunks to avoid parameter correlation.

REFERENCES

- [1] L. Poretsky, *Principles of Diabetes Mellitus*. New York, NY, USA: Springer, Jan. 2010.
- [2] B. Kovatchev, S. M. Anderson, D. Raghinaru, Y. C. Kudva, L. M. Laffel, C. Levy, J. E. Pinsky, R. P. Wadwa, B. Buckingham, F. J. Doyle, and S. A. Brown, “Randomized controlled trial of mobile closed-loop control,” *Diabetes Care*, vol. 43, no. 3, pp. 607–615, 2020.
- [3] Diabetes Control and Complications Trial Research Group, “The effect of intensive treatment of diabetes on the development and progression of long-term complications in insulin-dependent diabetes mellitus,” *New England J. Med.*, vol. 329, no. 14, pp. 977–986, 1993.
- [4] L. Bally, H. Thabit, and R. Hovorka, “Glucose-responsive insulin delivery for type 1 diabetes: The artificial pancreas story,” *Int. J. Pharmaceutics*, vol. 544, no. 2, pp. 309–318, Jun. 2018.
- [5] G. Sindelka, L. Heinemann, M. Berger, W. Frenck, and E. Chantelau, “Effect of insulin concentration, subcutaneous fat thickness and skin temperature on subcutaneous insulin absorption in healthy subjects,” *Diabetologia*, vol. 37, no. 4, pp. 377–380, Apr. 1994.
- [6] F. J. Doyle, L. M. Huyett, J. B. Lee, H. C. Zisser, and E. Dassau, “Closed-loop artificial pancreas systems: Engineering the algorithms,” *Diabetes Care*, vol. 37, no. 5, pp. 1191–1197, May 2014.
- [7] V. Naumova, S. V. Pereverzyev, and S. Sampath, “A meta-learning approach to the regularized learning—Case study: Blood glucose prediction,” *Neural Netw.*, vol. 33, pp. 181–193, Sep. 2012.
- [8] R. Gondhalekar, E. Dassau, and F. J. Doyle, III, “Periodic zone-MPC with asymmetric costs for outpatient-ready safety of an artificial pancreas to treat type 1 diabetes,” *Automatica*, vol. 71, pp. 237–246, Sep. 2016.
- [9] H. Kirchsteiger, R. Johansson, E. Renard, and L. D. Re, “Continuous-time interval model identification of blood glucose dynamics for type 1 diabetes,” *Int. J. Control*, vol. 87, no. 7, pp. 1454–1466, Jul. 2014.
- [10] N. Magdelaine, L. Chaillous, and C. H. Moog, “A long-term model of the glucose–insulin dynamics of type 1 diabetes,” *IEEE Trans. Biomed. Eng.*, vol. 62, no. 6, pp. 1546–1552, Jan. 2015.
- [11] Y. Ruan, M. E. Wilinska, H. Thabit, and R. Hovorka, “Modeling day-to-day variability of glucose–insulin regulation over 12-week home use of closed-loop insulin delivery,” *IEEE Trans. Biomed. Eng.*, vol. 64, no. 6, pp. 1412–1419, Jun. 2017.
- [12] B. Grosman, D. Wu, D. Miller, L. Lintreuer, A. Roy, N. Parikh, and F. R. Kaufman, “Sensor-augmented pump-based customized mathematical model for type 1 diabetes,” *Diabetes Technol. Therapeutics*, vol. 20, no. 3, pp. 207–221, Mar. 2018.
- [13] J. Garcia-Tirado, C. Zuluaga-Bedoya, and M. D. Breton, “Identifiability analysis of three control-oriented models for use in artificial pancreas systems,” *J. Diabetes Sci. Technol.*, vol. 12, no. 5, pp. 937–952, Sep. 2018.
- [14] C. E. Hann, J. G. Chase, J. Lin, T. Lotz, C. V. Doran, and G. M. Shaw, “Integral-based parameter identification for long-term dynamic verification of a glucose–insulin system model,” *Comput. Methods Programs Biomed.*, vol. 77, no. 3, pp. 259–270, Mar. 2005.

- [15] M. Messori, C. Toffanin, S. Del Favero, G. De Nicolao, C. Cobelli, and L. Magni, "Model individualization for artificial pancreas," *Comput. Methods Programs Biomed.*, vol. 171, no. 1, pp. 133–140, Apr. 2019.
- [16] C. Toffanin, S. Del Favero, E. M. Aiello, M. Messori, C. Cobelli, and L. Magni, "Glucose-insulin model identified in free-living conditions for hypoglycaemia prevention," *J. Process Control*, vol. 64, no. 1, pp. 27–36, Apr. 2018.
- [17] P. Soru, G. De Nicolao, C. Toffanin, C. Dalla Man, C. Cobelli, and L. Magni, "MPC based artificial pancreas: Strategies for individualization and meal compensation," *Annu. Rev. Control*, vol. 36, no. 1, pp. 118–128, Apr. 2012.
- [18] C. Toffanin, E. M. Aiello, C. Cobelli, and L. Magni, "Hypoglycemia prevention via personalized glucose-insulin models identified in free-living conditions," *J. Diabetes Sci. Technol.*, vol. 13, no. 6, pp. 1008–1016, Nov. 2019.
- [19] C. Toffanin, E. M. Aiello, S. Del Favero, C. Cobelli, and L. Magni, "Multiple models for artificial pancreas predictions identified from free-living condition data: A proof of concept study," *J. Process Control*, vol. 77, pp. 29–37, May 2019.
- [20] K. Turksoy, L. Quinn, E. Littlejohn, and A. Cinar, "Multivariable adaptive identification and control for artificial pancreas systems," *IEEE Trans. Biomed. Eng.*, vol. 61, no. 3, pp. 883–891, Mar. 2014.
- [21] C. Liu, J. Vehf, P. Avari, M. Reddy, N. Oliver, P. Georgiou, and P. Herrero, "Long-term glucose forecasting using a physiological model and deconvolution of the continuous glucose monitoring signal," *Sensors*, vol. 19, no. 19, p. 4338, Oct. 2019.
- [22] A. J. Laguna, P. Rossetti, F. J. Ampudia-Blasco, J. Vehf, and J. Bondia, "Identification of intra-patient variability in the postprandial response of patients with type 1 diabetes," *Biomed. Signal Process. Control*, vol. 12, no. 1, pp. 39–46, Jul. 2014.
- [23] A. J. Laguna, P. Rossetti, F. J. Ampudia-Blasco, J. Vehf, and J. Bondia, "Experimental blood glucose interval identification of patients with type 1 diabetes," *J. Process Control*, vol. 24, no. 1, pp. 171–181, Jan. 2014.
- [24] R.-E. Precup, T.-A. Teban, T. E. A. D. Oliveira, and E. M. Petriu, "Evolving fuzzy models for myoelectric-based control of a prosthetic hand," in *Proc. IEEE Int. Conf. Fuzzy Syst. (FUZZ-IEEE)*, Jul. 2016, pp. 72–77.
- [25] A. Albu, R. E. Precup, and T. A. Teban, "Results and challenges of artificial neural networks used for decision-making and control in medical applications," *Facta Universitatis, Mech. Eng.*, vol. 17, no. 3, pp. 285–308, 2019.
- [26] E. Balsa-Canto, A. A. Alonso, and J. R. Banga, "An iterative identification procedure for dynamic modeling of biochemical networks," *BMC Syst. Biol.*, vol. 4, no. 1, p. 11, Dec. 2010.
- [27] R. N. Bergman, Y. Z. Ider, C. R. Bowden, and C. Cobelli, "Quantitative estimation of insulin sensitivity," *Amer. J. Physiol.-Endocrinol. Metabolism*, vol. 236, no. 6, pp. E667–E677, Jun. 1979.
- [28] R. N. Bergman, L. S. Phillips, and C. Cobelli, "Physiologic evaluation of factors controlling glucose tolerance in man: Measurement of insulin sensitivity and beta-cell glucose sensitivity from the response to intravenous glucose," *J. Clin. Invest.*, vol. 68, no. 6, pp. 1456–1467, Dec. 1981.
- [29] V. W. Bolie, "Coefficients of normal blood glucose regulation," *J. Appl. Physiol.*, vol. 16, no. 5, pp. 783–788, Sep. 1961.
- [30] C. Cobelli, C. Dalla Man, G. Sparacino, L. Magni, G. De Nicolao, and B. P. Kovatchev, "Diabetes: Models, signals, and control," *IEEE Rev. Biomed. Eng.*, vol. 2, pp. 54–96, 2009.
- [31] E. D. Lehmann and T. Deutsch, "A physiological model of glucose-insulin interaction in type 1 diabetes mellitus," *J. Biomed. Eng.*, vol. 14, no. 3, pp. 235–242, May 1992.
- [32] J. T. Sorensen, "A physiologic model of glucose metabolism in man and its use to design and assess improved insulin therapies for diabetes," Ph.D. dissertation, Dept. Chem. Eng., Massachusetts Inst. Technol., Cambridge, MA, USA, 1985.
- [33] G. Steil, B. Clark, M. Kanderian, and K. Rebrin, "Modeling insulin action for development of a closed-loop artificial pancreas," *Diabetes Technol. Therapeutics*, vol. 7, no. 1, pp. 94–109, 2005.
- [34] C. Cobelli, G. Toffolo, and E. Ferrannini, "A model of glucose kinetics and their control by insulin, compartmental and noncompartmental approaches," *Math. Biosci.*, vol. 72, no. 2, pp. 291–315, Dec. 1984.
- [35] A. Caumo and C. Cobelli, "Hepatic glucose production during the labeled IVGTT: Estimation by deconvolution with a new minimal model," *Amer. J. Physiol.-Endocrinol. Metabolism*, vol. 264, no. 5, pp. E829–E841, May 1993.
- [36] P. Vicini, A. Caumo, and C. Cobelli, "The hot IVGTT two-compartment minimal model: Indexes of glucose effectiveness and insulin sensitivity," *Amer. J. Physiol.-Endocrinol. Metabolism*, vol. 273, no. 5, pp. 1024–1032, 1997.
- [37] G. Toffolo and C. Cobelli, "The hot IVGTT two-compartment minimal model: An improved version," *Amer. J. Physiol.-Endocrinol. Metabolism*, vol. 284, no. 2, pp. 317–321, 2003.
- [38] K. Krudys, M. Dodds, S. Nissen, and P. Vicini, "Integrated model of hepatic and peripheral glucose regulation for estimation of endogenous glucose production during the hot IVGTT," *Amer. J. Physiol.-Endocrinol. Metabolism*, vol. 288, no. 5, pp. 1038–1046, 2005.
- [39] A. De Gaetano and O. Arino, "Mathematical modelling of the intravenous glucose tolerance test," *J. Math. Biol.*, vol. 40, no. 2, pp. 136–168, Feb. 2000.
- [40] J. Li, Y. Kuang, and B. Li, "Analysis of IVGTT glucose-insulin interaction models with time delay," *Discrete Continuous Dyn. Syst. B*, vol. 1, no. 1, pp. 103–124, 2001.
- [41] J. Li, Y. Kuang, and C. C. Mason, "Modeling the glucose-insulin regulatory system and ultradian insulin secretory oscillations with two explicit time delays," *J. Theor. Biol.*, vol. 242, no. 3, pp. 722–735, Oct. 2006.
- [42] S. Panunzi, P. Palumbo, and A. De Gaetano, "A discrete single delay model for the intra-venous glucose tolerance test," *Theor. Biol. Med. Model.*, vol. 4, no. 1, p. 35, Dec. 2007.
- [43] P. G. Fabbietti, V. Canonico, M. O. Federici, M. M. Benedetti, and E. Sarti, "Control oriented model of insulin and glucose dynamics in type 1 diabetics," *Med. Biol. Eng. Comput.*, vol. 44, nos. 1–2, pp. 69–78, Mar. 2006.
- [44] T. Van Herpe, B. Pluymers, M. Espinoza, G. Van den Berghe, and B. De Moor, "A minimal model for glycemia control in critically ill patients," in *Proc. Int. Conf. IEEE Eng. Med. Biol. Soc.*, Aug. 2006, pp. 5432–5435.
- [45] J. G. Chase, G. M. Shaw, J. Lin, C. V. Doran, C. Hann, T. Lotz, G. C. Wake, and B. Broughton, "Targeted glycemic reduction in critical care using closed-loop control," *Diabetes Technol. Therapeutics*, vol. 7, no. 2, pp. 274–282, Apr. 2005.
- [46] J. G. Chase, G. M. Shaw, X. W. Wong, T. Lotz, J. Lin, and C. E. Hann, "Model-based glycaemic control in critical care—A review of the state of the possible," *Biomed. Signal Process. Control*, vol. 1, no. 1, pp. 3–21, Jan. 2006.
- [47] J. Lin, N. N. Razak, C. G. Pretty, A. Le Compte, P. Docherty, J. D. Parente, G. M. Shaw, C. E. Hann, and J. G. Chase, "A physiological intensive control insulin-nutrition-glucose (ICING) model validated in critically ill patients," *Comput. Methods Programs Biomed.*, vol. 102, no. 2, pp. 192–205, May 2011.
- [48] A. Roy and R. S. Parker, "Dynamic modeling of free fatty acid, glucose, and insulin: An extended 'minimal model,'" *Diabetes Technol. Therapeutics*, vol. 8, no. 6, pp. 617–626, Dec. 2006.
- [49] M. Fernández and D. P. Atherton, "Analysis of insulin sensitivity estimates from linear models of glucose disappearance," *Appl. Math. Comput.*, vol. 167, no. 1, pp. 528–538, Aug. 2005.
- [50] M. Fernandez, M. Villasana, and D. Streja, "Glucose dynamics in type I diabetes: Insights from the classic and linear minimal models," *Comput. Biol. Med.*, vol. 37, no. 5, pp. 611–627, May 2007.
- [51] S. S. Kanderian, S. Weinzimer, G. Voskanyan, and G. M. Steil, "Identification of intraday metabolic profiles during closed-loop glucose control in individuals with type 1 diabetes," *J. Diabetes Sci. Technol.*, vol. 3, no. 5, pp. 1047–1057, Sep. 2009.
- [52] R. Hovorka, F. Shojaee-Moradie, P. Carroll, L. Chassin, I. Gowrie, N. Jackson, R. Tudor, A. Margot Umpleby, and R. Jones, "Partitioning glucose distribution/transport, disposal, and endogenous production during IVGTT," *Amer. J. Physiol.-Endocrinol. Metabolism*, vol. 282, no. 5, pp. 992–1007, 2002.
- [53] R. Hovorka, V. Canonico, L. J. Chassin, U. Haueter, M. Massi-Benedetti, M. O. Federici, T. R. Pieber, H. C. Schaller, L. Schaupp, T. Vering, and M. E. Wilinska, "Nonlinear model predictive control of glucose concentration in subjects with type 1 diabetes," *Physiol. Meas.*, vol. 25, no. 4, pp. 905–920, Aug. 2004.
- [54] M. W. Percival, W. C. Bevier, Y. Wang, E. Dassau, H. C. Zisser, L. Jovanović, and F. J. Doyle, "Modeling the effects of subcutaneous insulin administration and carbohydrate consumption on blood glucose," *J. Diabetes Sci. Technol.*, vol. 4, no. 5, pp. 1214–1228, Sep. 2010.
- [55] M. W. Percival, Y. Wang, B. Grosman, E. Dassau, H. Zisser, L. Jovanović, and F. J. Doyle, "Development of a multi-parametric model predictive control algorithm for insulin delivery in type 1 diabetes mellitus using clinical parameters," *J. Process Control*, vol. 21, no. 3, pp. 391–404, Mar. 2011.

- [56] H. Kirchsteiger, G. C. Estrada, S. Pölzer, E. Renard, and L. del Re, "Estimating interval process models for type 1 diabetes for robust control design," in *Proc. 18th World Congr. Int. Fed. Autom. Control*, vol. 4, 2011, pp. 11761–11766.
- [57] H. Kirchsteiger, S. Polzer, R. Johansson, E. Renard, and L. del Re, "Direct continuous time system identification of MISO transfer function models applied to type 1 diabetes," in *Proc. IEEE Conf. Decis. Control Eur. Control Conf.*, Dec. 2011, pp. 5176–5181.
- [58] H. Kirchsteiger and L. del Re, "A model based bolus calculator for blood glucose control in type 1 diabetes," in *Proc. Amer. Control Conf.*, Jun. 2014, pp. 5465–5470.
- [59] D. Boiroux, A. Duun-Henriksen, S. Schmidt, K. Nørgaard, N. K. Poulsen, H. Madsen, and J. B. Jørgensen, "Assessment of model predictive and adaptive glucose control strategies for people with type 1 diabetes," *IFAC Proc. Volumes*, vol. 19, no. 3, pp. 231–236, 2014.
- [60] I. Ben Abbes, M. Lefebvre, H. Cormerais, and P. Richard, "A new model for closed-loop control in type 1 diabetes," *IFAC Proc. Volumes*, vol. 44, pp. 8360–8365, Jan. 2011.
- [61] A. György, L. Kovács, P. Szalay, D. Drexler, B. Beny, and Z. Beny, "Quasi-model-based control of type 1 diabetes mellitus," *J. Electr. Comput. Eng.*, vol. 2011, pp. 1–12, Jan. 2011.
- [62] T. Prud'homme, A. Bock, G. François, and D. Gillet, "Preclinically assessed optimal control of postprandial glucose excursions for type 1 patients with diabetes," in *Proc. IEEE Int. Conf. Autom. Sci. Eng.*, Aug. 2011, pp. 702–707.
- [63] A. K. Duun-Henriksen, S. Schmidt, R. M. Røge, J. B. Møller, K. Nørgaard, J. B. Jørgensen, and H. Madsen, "Model identification using stochastic differential equation grey-box models in diabetes," *J. Diabetes Sci. Technol.*, vol. 7, no. 2, pp. 431–440, Mar. 2013.
- [64] S. Schmidt, D. Boiroux, A. K. Duun-Henriksen, L. Frössing, O. Skyggebjerg, J. B. Jørgensen, N. K. Poulsen, H. Madsen, S. Madsbad, and K. Nørgaard, "Model-based closed-loop glucose control in type 1 diabetes: The DiaCon experience," *J. Diabetes Sci. Technol.*, vol. 7, no. 5, pp. 1255–1264, Sep. 2013.
- [65] P. Palumbo, S. Ditlevsen, A. Bertuzzi, and A. De Gaetano, "Mathematical modeling of the glucose–insulin system: A review," *Math. Biosci.*, vol. 244, no. 2, pp. 69–81, Aug. 2013.
- [66] A. Bock, G. François, and D. Gillet, "A therapy parameter-based model for predicting blood glucose concentrations in patients with type 1 diabetes," *Comput. Methods Programs Biomed.*, vol. 118, no. 2, pp. 107–123, Feb. 2015.
- [67] D. Lv, M. D. Breton, and L. S. Farhy, "Pharmacokinetics modeling of exogenous glucagon in type 1 diabetes mellitus patients," *Diabetes Technol. Therapeutics*, vol. 15, no. 11, pp. 935–941, Nov. 2013.
- [68] S. L. Wendt, A. Ranjan, J. K. Møller, S. Schmidt, C. B. Knudsen, J. J. Holst, S. Madsbad, H. Madsen, K. Nørgaard, and J. B. Jørgensen, "Cross-validation of a glucose-insulin-glucagon pharmacodynamics model for simulation using data from patients with type 1 diabetes," *J. Diabetes Sci. Technol.*, vol. 11, no. 6, pp. 1101–1111, Nov. 2017.
- [69] S. M. Ewings, S. K. Sahu, J. J. Valletta, C. D. Byrne, and A. J. Chipperfield, "A Bayesian network for modelling blood glucose concentration and exercise in type 1 diabetes," *Stat. Methods Med. Res.*, vol. 24, no. 3, pp. 342–372, Jun. 2015.
- [70] L. Lema-Perez, E. Aguirre-Zapata, and J. Garcia-Tirado, "Recent advances in mathematical models for the understanding and treatment of type 1 diabetes mellitus," in *Proc. IEEE 2nd Colombian Conf. Autom. Control (CCAC)*, Oct. 2015, pp. 1–6.
- [71] T. MohammadRidha, P. S. Rivadeneira, M. Cardelli, N. Magdelaine, and C. H. Moog, "Towards hypoglycemia prediction and avoidance for type 1 diabetic patients," in *Proc. IEEE 56th Annu. Conf. Decis. Control (CDC)*, Dec. 2017, pp. 4118–4123.
- [72] F. García-García, R. Hovorka, M. E. Wilinska, D. Elleri, and M. E. Hernando, "Modelling the effect of insulin on the disposal of meal-attributable glucose in type 1 diabetes," *Med. Biol. Eng. Comput.*, vol. 55, no. 2, pp. 271–282, Feb. 2017.
- [73] D. Boiroux, M. Hagdrup, Z. Mahmoudi, N. Poulsen, H. Madsen, and J. Jørgensen, "Model identification using continuous glucose monitoring data for type 1 diabetes," *IFAC-PapersOnLine*, vol. 49, no. 7, pp. 759–764, 2016.
- [74] D. Boiroux, M. Hagdrup, Z. Mahmoudi, N. K. Poulsen, H. Madsen, and J. B. Jørgensen, "An ensemble nonlinear model predictive control algorithm in an artificial pancreas for people with type 1 diabetes," in *Proc. Eur. Control Conf. (ECC)*, Jun. 2016, pp. 2115–2120.
- [75] A. Nath, S. Biradar, A. Balan, R. Dey, and R. Padhi, "Physiological models and control for type 1 diabetes mellitus: A brief review," *IFAC-PapersOnLine*, vol. 51, no. 1, pp. 289–294, 2018.
- [76] S. Oviedo, J. Vehí, R. Calm, and J. Armengol, "A review of personalized blood glucose prediction strategies for T1DM patients," *Int. J. Numer. Methods Biomed. Eng.*, vol. 33, no. 6, p. e2833, Jun. 2017.
- [77] P. Colmegna, R. S. Sánchez-Peña, and R. Gondhalekar, "Linear parameter-varying model to design control laws for an artificial pancreas," *Biomed. Signal Process. Control*, vol. 40, pp. 204–213, Feb. 2018.
- [78] M. Moscoso-Vasquez, P. Colmegna, and R. S. Sanchez-Pena, "Control-oriented model including hyperinsulinemia induced insulin resistance in type 1 diabetes," in *Proc. IEEE 4th Colombian Conf. Autom. Control (CCAC)*, Oct. 2019, pp. 1–6.
- [79] H. Ali, W. Boutayeb, A. Boutayeb, and N. Merabet, "Parameter estimation of a meal glucose–insulin model for T1DM patients from therapy historical data," in *Proc. 8th Int. Conf. Modeling Simulation Appl. Optim. (ICMSAO)*, 2019, pp. 8–11.
- [80] G. C. Goodwin, A. M. Medioli, D. S. Carrasco, B. R. King, and Y. Fu, "A fundamental control limitation for linear positive systems with application to type 1 diabetes treatment," *Automatica*, vol. 55, pp. 73–77, May 2015.
- [81] N. Jeandidier, J. P. Riveline, and N. Tubiana-Rufi, "Treatment of diabetes mellitus using an external insulin pump in clinical practice," *Diabetes Metabolism*, vol. 34, no. 4, pp. 38–425, 2008.
- [82] J. Walsh, R. Roberts, and T. Bailey, "Guidelines for insulin dosing in continuous subcutaneous insulin infusion using new formulas from a retrospective study of individuals with optimal glucose levels," *J. Diabetes Sci. Technol.*, vol. 4, no. 5, pp. 1174–1181, Sep. 2010.
- [83] B. W. Bode, J. Kyllö, and F. R. Kaufman, "Pumping protocol: A guide to insulin pump therapy initiation," in *Medtronic*. Northridge, CA, USA: Medtronic, 2012.
- [84] A. F. Villaverde, "Observability and structural identifiability of nonlinear biological systems," *Comput. Methods Identificat. Model. Complex Biol. Syst.*, vol. 2019, Jan. 2019, Art. no. 8497093.
- [85] A. Raue, C. Kreutz, T. Maiwald, J. Bachmann, M. Schilling, U. Klingmüller, and J. Timmer, "Structural and practical identifiability analysis of partially observed dynamical models by exploiting the profile likelihood," *Bioinformatics*, vol. 25, no. 15, pp. 1923–1929, Aug. 2009.
- [86] O. Chiş, J. R. Banga, and E. Balsa-Canto, "GenSSI: A software toolbox for structural identifiability analysis of biological models," *Bioinformatics*, vol. 27, pp. 1–2610, Jul. 2011.
- [87] O.-T. Chis, J. R. Banga, and E. Balsa-Canto, "Structural identifiability of systems biology models: A critical comparison of methods," *PLoS ONE*, vol. 6, no. 11, Nov. 2011, Art. no. e27755.
- [88] M. Rodríguez-Fernandez, J. Banga, and F. J. Doyle, III, "Novel global sensitivity analysis methodology accounting for the crucial role of the distribution of input parameters: Application to systems biology models," *Int. J. Robust Nonlinear Control*, vol. 22, pp. 1082–1102, Jul. 2012.
- [89] R. Brun, P. Reichert, and H. R. Künsch, "Practical identifiability analysis of large environmental simulation models," *Water Resour. Res.*, vol. 37, no. 4, pp. 1015–1030, Apr. 2001.
- [90] T. Söderström and P. Stoica, *System Identification*. Upper Saddle River, NJ, USA: Prentice-Hall, 1989.
- [91] C. D. Man, F. Micheletto, D. Lv, M. Breton, B. Kovatchev, and C. Cobelli, "The UVA/PADOVA type 1 diabetes simulator: New features," *J. Diabetes Sci. Technol.*, vol. 8, no. 1, pp. 26–34, Jan. 2014.

• • •